

Cite this: DOI: 10.1039/c0ee00723d

www.rsc.org/ees

## COMMUNICATION

### Polar interface-induced improvement in high photocatalytic hydrogen evolution over ZnO–CdS heterostructures†

Xuewen Wang,<sup>ab</sup> Lichang Yin,<sup>ac</sup> Gang Liu,<sup>a</sup> Lianzhou Wang,<sup>b</sup> Riichiro Saito,<sup>c</sup> Gao Qing (Max) Lu<sup>\*b</sup> and Hui-Ming Cheng<sup>\*a</sup>

Received 29th November 2010, Accepted 17th August 2011

DOI: 10.1039/c0ee00723d

**ZnO surfaces are mainly covered by two polar facets and six nonpolar facets. Due to the unique advantage of polar facets in promoting interface charge carrier transfer in ZnO–CdS heterostructures, the hydrogen evolution rate over ZnO disk–CdS nanoparticle heterostructures is 2.8 times that of the ZnO rod–CdS nanoparticle one.**

Photocatalytic hydrogen evolution over inorganic semiconductor photocatalysts under solar light has attracted increasing attention in research due to its potential in renewable energy development.<sup>1–5</sup> Heterostructuring of different photocatalysts, which has advantages in promoting the separation of photoexcited electrons and holes and extending the light absorption range, is playing an increasingly important role in improving photocatalytic hydrogen evolution efficiency.<sup>6–14</sup> A solid interfacial structure is a key factor in determining charge carrier transfer behavior between different semiconductors in heterostructures and thus the performance of heterostructured photocatalysts.<sup>6–14</sup> Developing various photocatalysts with defined crystal

facets has attracted much attention since the realization of anatase TiO<sub>2</sub> with a large percentage of {001} facets.<sup>15–17</sup> Photoreactivities of materials are affected by different percentages of facets with different atomic configurations and coordination numbers. ZnO with an excellent electron transport capability is a potential candidate as a highly efficient photocatalyst for hydrogen evolution.<sup>6–11</sup> The most successful systems developed so far consist of ZnO–GaN solid solution photocatalysts.<sup>1</sup> Compared to other metal oxides, one distinct feature of ZnO hexagonal rods is the presence of two Zn-terminated (0001) and O-terminated (000 $\bar{1}$ ) polar surfaces at the two ends of the rods.<sup>18</sup> Recent results reveal that a higher percentage of polar surfaces in ZnO disks lead to a higher photocatalytic activity.<sup>19–21</sup> This higher activity is due to the favorable surface separation and transfer of photoexcited electrons and holes. Inspired by these results, we hypothesize that polar surfaces may be important in ZnO based heterostructures, which has never been considered, to our knowledge.

In this study, two groups of hexagonal ZnO disks and rods, which are mainly enclosed with different percentages of two polar facets (top (000 $\bar{1}$ ) and bottom (0001)), and six nonpolar side-facets were prepared. To elucidate the role of the polar interface in affecting electron transfer, CdS nanoparticles (NPs) were subsequently deposited onto these disks and rods to form ZnO–CdS heterostructures. Very encouragingly, the photocatalytic activity measurements indeed indicate a positive role of the polar interface to improve hydrogen evolution rate by a factor of 2.8. By first-principles calculations, the origin of such improvement is elucidated.

Hexagonal ZnO disks were synthesized by a hydrothermal route. 40 mL of aqueous solution containing 0.5 M zinc acetate and 0.1 M sodium hydroxide in an autoclave was heated at 120 °C for 20 h. The

<sup>a</sup>Shenyang National Laboratory for Materials Science Institute of Metal Research, Chinese Academy of Sciences, 72<sup>#</sup> Wenhua RD, Shenyang, 110016, P. R. China. E-mail: cheng@imr.ac.cn; Fax: (+86) 24 2390 3126

<sup>b</sup>ARC Centre of Excellence for Functional Nanomaterials, The University of Queensland, QLD 4072, Australia. E-mail: maxlu@uq.edu.au; Fax: (+) 61 7 33653735

<sup>c</sup>Department of Physics, Tohoku University, Sendai, 980-8578, Japan

† Electronic supplementary information (ESI) available: XRD patterns, XPS, SEM and TEM images, photocatalytic activity, and schematic side view of the geometries of ZnO. See DOI: 10.1039/c0ee00723d

#### Broader context

Photocatalytic hydrogen evolution over semiconductors utilizing solar light is becoming a significant subject to solve the energy problem. In the photocatalytic process, significant photocatalytic carriers separation and electron transfer could be improved by polar facets. ZnO surfaces are covered by polar and nonpolar facets. We developed a hydrothermal route for synthesizing hexagonal ZnO disks with dominant Zn-terminated (0001) and O-terminated (000 $\bar{1}$ ) polar facets of high quality. Compared to that of ZnO rod–CdS nanoparticle heterostructures, the ZnO disk after loading CdS nanoparticles exhibits a higher photocatalytic hydrogen evolution rate due to photoexcited electron/hole separation enhanced by polar interfaces. Furthermore, by first-principles calculations, the origin of such an improvement is explored. This polar interfaces study will shed light on heterostructured photocatalyst designation.

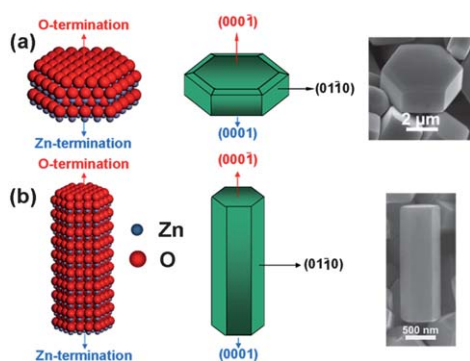


**Fig. 1** Atomic models, schematics and SEM images of a hexagonal ZnO (a) disk and (b) rod.

percentage of polar facets in hexagonal ZnO disks can be controlled by changing the concentration of NaOH: the lower the NaOH concentration, the higher the percentage of polar facets (Fig. S1†). Atomic models, schematics and scanning electron microscopy (SEM) images of ZnO disks and rods are shown in Fig. 1. The top surface of hexagonal ZnO particles is an O-terminated (0001) facet with negative charge. On the contrary, the bottom (0001) facet is positively charged by the terminated Zn atoms. The sides of disks and rods are enclosed by (0110), (01̄10), (1100), (1̄100), (1010) and (1̄010) nonpolar facets with alternating O- and Zn-termination on the flanks. Due to the shrinking of O atoms on the top (0001) facet, small oblique facets connecting the (0001) facet and the edges of nonpolar facets (Fig. 1a) are formed. The morphology of ZnO disks is very similar to what is predicted by an atomic model. Compared to ZnO rods with dominant nonpolar facets, hexagonal ZnO disks are enclosed by dominant polar facets making it possible to explore the effects of polar and nonpolar facets in the photocatalytic activity of ZnO.

Typical SEM images of ZnO disks and rods are shown in Fig. 2a and c. Their XRD patterns can be assigned to hexagonal ZnO (Fig. S2†). Compared to ZnO rods (Fig. 2c) being *ca.* 0.6 μm in diameter and *ca.* 3 μm in length, the average diameter and thickness of ZnO disks are *ca.* 4.5 μm and *ca.* 1.7 μm respectively (Fig. 2a). ZnO disks have smooth surfaces and sharp edges (Fig. 2a and S3†), where the average percentage of (0001) and (0001̄) facets is *ca.* 51%. After coating with 5 wt% CdS by CVD, CdS NPs are uniformly deposited on the ZnO surfaces (Fig. 2b and 2d). A close contact between ZnO disks/rods and CdS NPs is indicated by the obvious shifts in the binding energies of Zn-2p, O-1s, Cd-3d, and S-2p in ZnO–CdS heterostructures compared to those in pristine ZnO or CdS (Fig. S4). The intimate contact between CdS and ZnO can also be seen from the TEM images of ZnO disk–CdS NP heterostructures shown in Fig. 2e and 2f. CdS NPs on the ZnO disk are highly crystalline (Fig. 2g).

Due to different surface atomic configurations between the polar and nonpolar facets, the disks show a marginal blue shift of the absorption edge by *ca.* 10 nm compared to the rods (Fig. 3a). The derived bandgap is increased by *ca.* 0.08 eV. XPS valence band (VB) spectra reveal that the VB maximum of the disks is lower than that of the rods, which indicates that stronger oxidative holes are generated on the disks (Fig. 3b). After loading CdS NPs, ZnO could mainly act as an oxidative site while CdS could act as a reductive site for hydrogen evolution,<sup>6</sup> therefore, the photocatalytic activity of the

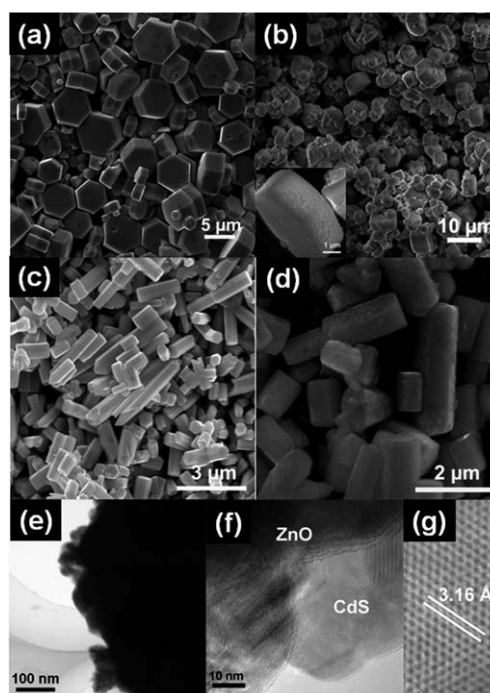


**Fig. 2** SEM images of hexagonal ZnO (a) disks and (c) rods, (b) disks and (d) rods coated with 5 wt% CdS NPs; TEM images of (e) CdS NPs on a ZnO disk, (f) its interface, and (g) a high resolution TEM image of a CdS NP on a ZnO disk.

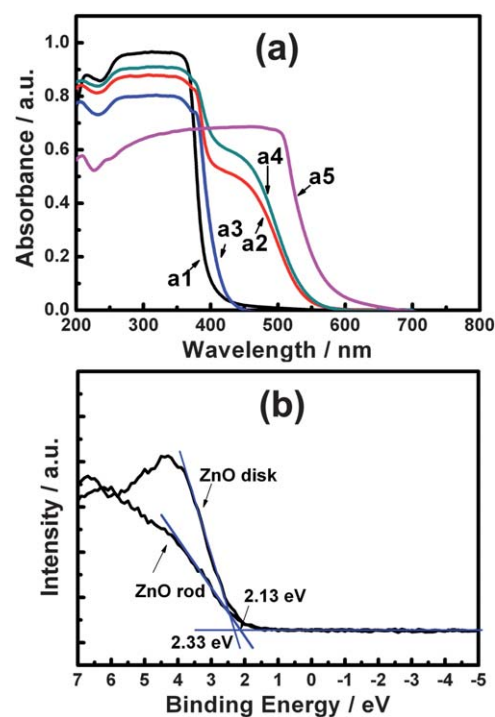
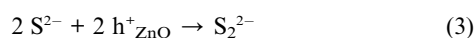
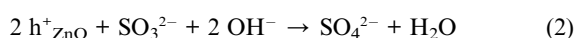
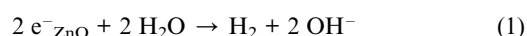


**Fig. 3** (a) UV-visible absorption spectra of (a1) ZnO disks and (a2) those after coating with 5 wt% CdS, (a3) ZnO rods and (a4) those after coating with 5 wt% CdS, and (a5) solely CdS; (b) total densities of states of XPS valence band spectra of ZnO disks and rods.

system will be improved because of ZnO disks with a stronger oxidative power. A similar phenomenon was also reported in anatase TiO<sub>2</sub> photocatalysts with different percentages of {001} and {101} facets.<sup>22</sup> As a result of CdS coating, the absorption edges of the heterostructures were extended to *ca.* 550 nm (Fig. 3a).

Before examining the effect of the polar interfaces on the photocatalytic performance of the heterostructures, we first evaluated the photocatalytic hydrogen evolution from bare ZnO disks with different ratios of (0001) and (000 $\bar{1}$ ) polar facets and ZnO rods. It is found that photocatalytic hydrogen evolution of ZnO disks increased with increasing polar facet ratio, though the improvement is very small (See Table S1). As given in Table 1, there is only a marginal difference in the hydrogen evolution rates between the rod and disk samples. This result is not similar to what would be expected from the great role of the polar interface in significantly promoting the photodecomposition of organic pollutants.<sup>19,20</sup> Two possible reasons for this difference are suggested. One is that the polar function of the pristine ZnO disks is restrained because ZnO polar facets with charges could absorb ions in the reaction solution containing cations (Na<sup>+</sup>) and anions (S<sup>2-</sup> and SO<sub>3</sub><sup>2-</sup>). The other is that ZnO itself is not a good photocatalyst for hydrogen evolution due to its relatively low stability and the bottom of its conduction band (CB) being a little higher than H<sup>+</sup>/H<sub>2</sub> potential.<sup>23</sup>

The big difference in photocatalytic hydrogen evolution rates between the ZnO disk–CdS NP and the ZnO rod–CdS NP heterostructures can be understood from their different interface structures. The positively charged Zn-terminated (0001) and negatively charged O-terminated (000 $\bar{1}$ ) facets are expected to be more favorable for promoting interface charge carrier transfer in the heterostructures in contrast to the nonpolar (01 $\bar{1}$ 0) facet. Now it is useful to discuss charge carrier transfer processes in the heterostructures. Two possible mechanisms might exist in the ZnO–CdS heterostructures upon light excitation. One is a conventional mechanism that the photoexcited electrons flow from CdS with a higher CB edge to ZnO with a lower CB edge, and the holes transfer from ZnO with a lower VB edge to CdS with a higher VB edge. The subsequent photocatalytic reactions will occur as follows:



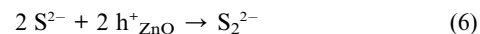
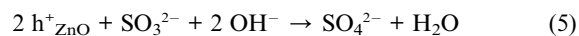
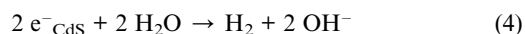
The other is the Z-scheme mechanism, where the photoexcited electrons from ZnO will directly recombine with the holes from CdS in

**Table 1** Comparison of specific surface areas and photocatalytic H<sub>2</sub> evolution rates of the bare ZnO disks and rods and the ones coated with 5 wt% CdS NPs

Samples	Specific Surface Area (m <sup>2</sup> g <sup>-1</sup> )	Hydrogen Evolution <sup>a</sup> . (μmol h <sup>-1</sup> )
ZnO disk	1.4	15.6
ZnO disk–CdS	10.9	88.6
ZnO rod	2.2	11.2
ZnO rod–CdS	12.5	31.2

<sup>a</sup> Measurement conditions: 0.1 g of sample, 300 mL of aqueous solution containing 0.1 M Na<sub>2</sub>S and 0.1 M Na<sub>2</sub>SO<sub>3</sub>, and a light source of 300 W Xe lamp.

the interface. The left electrons on CdS and holes on ZnO will induce the reduction (H<sub>2</sub> evolution) and oxidation reactions, respectively, as follows:



Considering the very low hydrogen evolution rate of the ZnO disk–CdS NPs under only visible light irradiation and the pure ZnO with low CB edge, it is reasonably believed that the second transfer mechanism might be dominant.

To better understand the effect of the ZnO surface state on photocatalysis, we performed first-principles calculations on the electronic properties for the top, bottom, and side surfaces of a ZnO crystal. A CdS crystal in the ZnO–CdS heterostructure serves to enhance the photocatalytic activity, therefore, here we did not consider the effect of the CdS crystal for simplicity. The calculated electronic densities of states (DOS) of the two polar (0001) and (000 $\bar{1}$ ) surfaces, and one nonpolar surface, (01 $\bar{1}$ 0), are shown in Fig. 4. Both the (0001) and (000 $\bar{1}$ ) polar surfaces are predicted to be metallic, while the nonpolar (01 $\bar{1}$ 0) surface remains semiconducting. The metallic nature of the surfaces arises from different causes based on the partial DOS analysis. The partial DOS of O-2p, Zn-4s, and Zn-3d for each surface are shown in the Fig. 4 insets. For the top (000 $\bar{1}$ ) surface, the metallic characteristic of the ZnO (000 $\bar{1}$ ) surface is mainly due to the highly dispersed Zn-4s orbital around the Fermi level, while the ZnO (000 $\bar{1}$ ) surface mainly consists of the O-2p orbital, reflecting the surface atom of each surface. The metallic features of both polar surfaces make charge transfer in the interface between ZnO and CdS feasible, which may enhance the photocatalytic performance of ZnO with larger polar surfaces. Therefore, (0001) and (000 $\bar{1}$ ) facets with polarity, metallic surfaces contribute to higher hydrogen evolution over the ZnO disk–CdS NP heterostructures.

In summary, hexagonal ZnO disks with dominant Zn-terminated (0001) and O-terminated (000 $\bar{1}$ ) polar facets were synthesized by a hydrothermal route. It was found that these polar facets can promote the interface charge carrier separation, and effective carrier

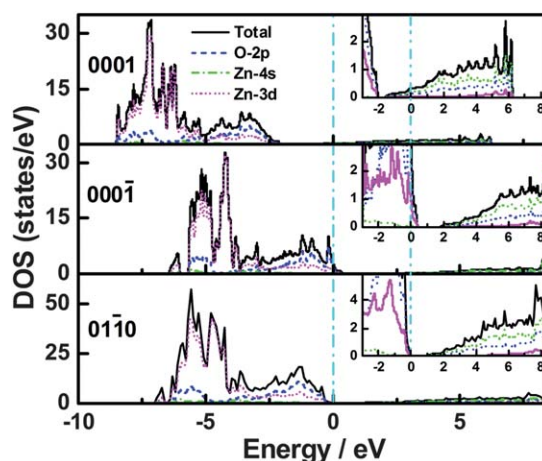


**Fig. 4** The calculated electronic density of states (DOS) of (0001), (000 $\bar{1}$ ), and (01 $\bar{1}$ 0) surfaces.

transfer was also observed in the ZnO disk–CdS NP heterostructures. As a result, the photocatalytic hydrogen evolution rate of the ZnO disk–CdS NP heterostructure is significantly improved.

## Acknowledgements

The financial support from the Major Basic Research Program, Ministry of Science and Technology China (No. 2009CB220001), NSF of China (Nos. 50921004, 51002160, 21090343, 51172243), Solar Energy Initiative and the Funding (KJXC2-YW-H21–01) of the Chinese Academy of Sciences, MOF Grants ZDYZ2008-2-A12, and Australian Research Council through its Centre's grant and DP0666345 is gratefully acknowledged. GL thanks the IMR SYNL-T.S. Kê Research Fellowship.

## Reference and notes

- 1 K. Maeda, K. Teramura, D. L. Lu, T. Takata, N. Saito, Y. Inoue and K. Domen, *Nature*, 2006, **440**, 295.
- 2 A. Kudo and Y. Miseki, *Chem. Soc. Rev.*, 2009, **38**, 253–278.
- 3 F. E. Osterloh, *Chem. Mater.*, 2008, **20**, 35–54.
- 4 X. C. Wang, K. Maeda, A. Thomas, K. Takanabe, G. Xin, J. M. Carlsson, K. Domen and M. Antonietti, *Nat. Mater.*, 2009, **8**, 76–80.
- 5 X. W. Wang, G. Liu, Z. G. Chen, F. Li, G. Q. Lu and H. M. Cheng, *Electrochem. Commun.*, 2009, **11**, 1174–1178.
- 6 X. W. Wang, G. Liu, Z. G. Chen, F. Li, L. Z. Wang, G. Q. Lu and H. M. Cheng, *Chem. Commun.*, 2009, 3452–3454.
- 7 X. W. Wang, G. Liu, Z. G. Chen, F. Li, G. Q. Lu and H. M. Cheng, *J. Mater. Res.*, 2010, **25**, 39–44.
- 8 X. W. Wang, G. Liu, G. Q. Lu and H. M. Cheng, *Int. J. Hydrogen Energy*, 2010, **35**, 8199–8205.
- 9 N. Chouhan, C. L. Yeh, S. F. Hu, J. H. Huang, C. W. Tsai, R. S. Liu, W. S. Chang and K. H. Chen, *J. Electrochem. Soc.*, 2010, **157**, B1430–B1433.
- 10 H. M. Chen, C. K. Chen, Y. C. Chang, C. W. Tsai, R. S. Liu, S. F. Hu, W. S. Chang and K. H. Chen, *Angew. Chem. Int. Ed.*, 2010, **49**, 5966–5969.
- 11 F. Xu, V. Volkov, Y. M. Zhu, H. Y. Bai, A. Rea, N. V. Valappil, W. Su, X. Y. Gao, I. L. Kuskovsky and H. Matsui, *J. Phys. Chem. C*, 2009, **113**, 19419–19423.
- 12 J. Zhang, Q. Xu, Z. Feng, M. Li and C. Li, *Angew. Chem., Int. Ed.*, 2008, **47**, 1766–1769.
- 13 G. Liu, L. Z. Wang, H. G. Yang, H. M. Cheng and G. Q. Lu, *J. Mater. Chem.*, 2010, **20**, 831–843.
- 14 H. Tada, T. Mitsui, T. Kiyonaga, T. Akita and K. Tanaka, *Nat. Mater.*, 2006, **5**, 782–786.
- 15 H. G. Yang, C. H. Sun, S. Z. Qiao, J. Zou, G. Liu, S. C. Smith, H. M. Cheng and G. Q. Lu, *Nature*, 2008, **453**, 638–U4.
- 16 G. Liu, H. G. Yang, X. W. Wang, L. N. Cheng, J. Pan, G. Q. Lu and H. M. Cheng, *J. Am. Chem. Soc.*, 2009, **131**, 12868–12869.
- 17 L. Q. Mai, Y. H. Gu, C. H. Han, B. Hu, W. Chen, P. C. Zhang, L. Xu, W. L. Guo and Y. Dai, *Nano Lett.*, 2009, **9**, 826–830.
- 18 G. Bruno, M. M. Giangregorio, G. Malandrino, P. Capezzuto, I. L. Fragala and M. Losurdo, *Adv. Mater.*, 2009, **21**, 1700–1706.
- 19 A. McLaren, T. Valdes-Solis, G. Q. Li and S. C. Tsang, *J. Am. Chem. Soc.*, 2009, **131**, 12540–12541.
- 20 J. H. Zeng, B. B. Jin and Y. F. Wang, *Chem. Phys. Lett.*, 2009, **472**, 90–95.
- 21 E. S. Jang, J. H. Won, S. J. Hwang and J. H. Choy, *Adv. Mater.*, 2006, **18**, 3309–3312.
- 22 G. Liu, C. H. Sun, H. G. Yang, S. C. Smith, L. Z. Wang, G. Q. Lu and H. M. Cheng, *Chem. Commun.*, 2010, **46**, 755–757.
- 23 U. Rau and M. Schmidt, *Thin Solid Films*, 2001, **387**, 141–146.